EVALUATION OF INFRASONIC SPATIAL FILTERS

Michael A.H. Hedlin, Jon Berger and Mark Zumberge

Institute of Geophysics and Planetary Physics
University of California, San Diego

Sponsored by Defense Threat Reduction Agency

ABSTRACT

The infrasound element of the global International Monitoring System (IMS) will consist of 60 stations. Each station in the global network will consist of an array of sensors. As the local surface wind strongly influences ambient infrasonic noise levels in the band of interest to the nuclear treaty monitoring community (between 0.05 and 4 Hz), each of these sensors will include a spatial filter designed to reduce the effects of wind noise. There are, however, many different design suggestions for spatial filtering system. In order to maximize the signal-to-noise ratio of signals of interest, it is essential that the spatial noise reduction systems be optimized to provide the most significant noise power reduction over the broadest band possible. We believe that substantial progress in these areas requires the comparative testing of the major noise reducing systems exposed to the same meteorological conditions.

Under our new DTRA contract we will construct and test several spatial filtering systems by simultaneous operation at the Pinon Flat Observatory (PFO) in southern California. These systems include the wind fence, microporous pipes, and a recent design in which a large number of open ports are connected to a summing manifold, and then to the microbarometer, by solid pipes. We will also compare these mechanical noise suppression schemes with a new design based on light-speed pressure averaging via optical fibres. The observatory is an ideal test site as it is subjected to winds that come from all azimuths at speeds ranging from 0 to over10 m/s.

Key Words: spatial averaging, turbulence

OBJECTIVE

Our objective is to evaluate several infrasonic noise reducing devices together at the Pinon Flat Observatory in southern California to identify which devices appear to be most effective under what circumstances.

BACKGROUND

Wind and Infrasonic Noise

The turbulent flow of wind is the most significant source of infrasonic noise in the band from .01 to 1 Hz (McDonald et al., 1971). The relationship between wind and infrasonic noise is given by Bernoulli s principle

$$p + (\rho v^2)/2 = C$$

where p is pressure, ρ is density, v is wind velocity and C is a constant. Differentiation of this formula shows that there is a simple linear scaling between variations in wind speed and pressure. Understanding the frequency dependence of infrasonic noise requires knowledge of the interaction of wind with topographic irregularities that cause the turbulence. In general terms, atmospheric turbulence is concentrated near the Earth s surface in the Atmospheric Boundary Layer (ABL; Kaimal and Finnigan, 1994) - a region of high Reynolds-number flow. The upper extent of the ABL is limited by the capping inversion which is highest (at 1 to 2 km) during the day when the Earth s surface radiates heat and lowest (10 s of meters) or nonexistent during the night (Panofsky and Dutton, 1984; Kaimal and Finnigan, 1994). The thickness of the boundary layer is also governed to some extent by topography as the turbulence of wind flow over the ground is increased by ground roughness. Large-scale atmospheric turbulence is maintained by thermal plumes and thus is most evident during the day. Wind shear introduces smaller eddies and cascades ener gy from the low to the higher frequencies (Kaimal and Finnigan, 1994). There is no universal statistical characterization of atmospheric turbulence at large scales (Wilson et al., 1999). The turbulence depends on the velocity and density profiles of the atmosphere as well as boundary effects such as topography and ground cover. The spatial structure of the atmospheric turbulence is dependent on the interaction of the wind with topography and can be modeled using one of a number of models including Gaussian, von Karman or Kolmogorov spectral models (Wilson et al., 1999). Wind noise is known to be incoherent at spacing of 10s of meters (e.g. Priestley, 1966). There exists a direct scaling between the size of the wind eddies and the time-frequency of the noise they produce. At 0.25 Hz, the scale of the turbulence is ~ 25 m (Grover, 1971). At comparable time frequencies, signals from remote sources have wavelengths that are considerably longer than any noise suppression device currently being considered. Thus, spatial averaging is expected to attenuate local sources of infrasonic noise while leaving signals from remote sources relatively unaltered.

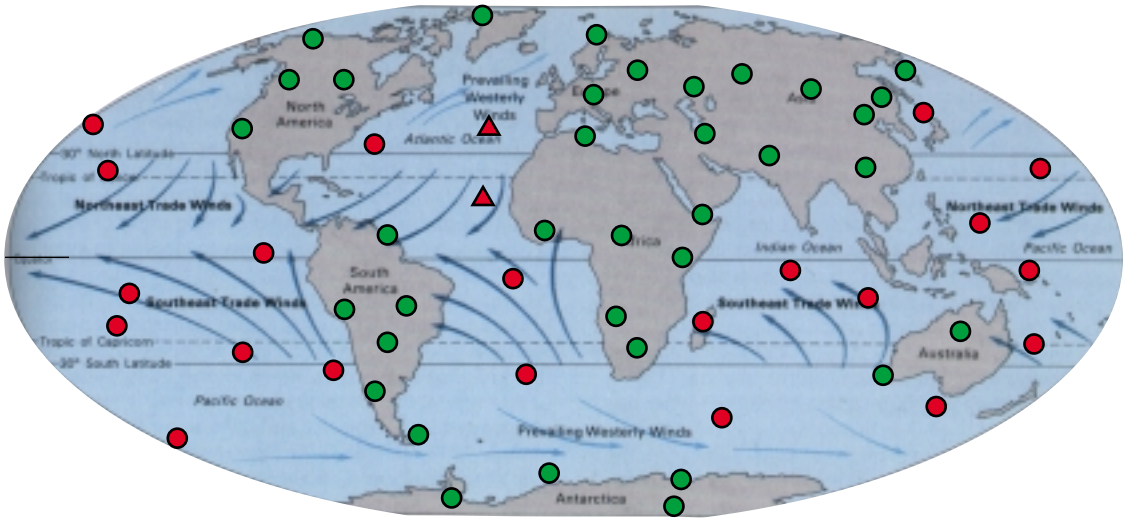

FIGURE 1. The planned global IMS infrasound network. Stations located on islands will, in general, be subject to strong winds and thus high infrasonic noise levels. Strong trade winds dominate in the tropics. In latitudes above 30°N and below 30°S the prevailing westerly winds dominate although local winds can be strongly influenced by local pressure cells. The 2 triangles in the Atlantic from north to south are the Azores and Cape Verde. Data from these sites is used in this paper. The background display of oceanic winds is adapted from the World Book. Encyclopedia.

Our group at IGPP recently collected infrasound and meteorological data on 3 islands in the Atlantic; Sao Miguel, Azores, Maio, Cape Verde and Ascension island. The experiments were conducted to collect infrasonic noise data required to make an informed recommendation about which site on each of these islands would be most suitable for a permanent IMS infrasound array. The experiments provided an abundance of data that is relevant to the issue of wind and infrasonic noise. Rudimentary spatial filters constructed with "spider" arms of perforated hose as illustrated in Figure 2 were used in these experiments.

In Figure 3 we display meteorological and infrasonic pressure data recorded in the Azores during a 15 minute time span in one mid-afternoon in October, 1998. The unfiltered pressure time series from the station at this site exhibits 30 second period fluctuations superimposed on substantially longer period energy. The shorter period variations dominate the filtered record (second panel from top). In this time period, minor wind velocity fluctuations are constant. The temperature and humidity vary relatively slowly. The detailed structure of the filtered pressure record results from the superposed contributions of myriad atmospheric phenomena.

The spectral content of the filtered data is displayed in Figure 4 which shows the decay in power levels from the peak at 30 second to the corner of the anti-aliasing filter at 9 Hz. A strong microbarom peak is centered at 0.2 Hz. The overall spectral shape is due to a well known phenomena in the atmosphere which receives a major input of energy at ~ 0.1 to 1 mHz. Energy from large scale eddies cascades into smaller eddies, and thus into higher frequencies, as the large eddies are broken up (Kaimal and Finnigan, 1994). The fall-off of energy below 0.01 Hz is due to the sensor filter.

From the spectral estimates taken over ~3 week time spans on each of the islands in the Atlantic we were able to investigate the dependence of infrasonic noise on wind speed at frequencies from 0.02 to 5 Hz. In the left panel of Figure 5 we display average power spectral density as a function of wind speed at a site on Maio, Cape Verde (Figure 1). Each curve from lowest to highest comes from a wind speed bin that spans 0.5 m/s. The first bin includes data from 0 to 0.5 m/s, the second from 0.5 to 1.0, and so on up to 3 m/s. When the wind speed is below 0.5 m/s the microbarom peak is obvious. At higher wind conditions the peak becomes obscured. At all frequencies the infrasonic power increases with increasing wind speed; the power increase is most evident at the long periods.

The right panel of this figure shows power spectral estimates from narrow frequency bands centered at the frequencies listed at the extreme right. The dependence of infrasonic power on wind speed and on frequency is clear. At this location in the northern trades, the wind is from the northeast and as a result the dependence of infrasound power on wind speed is relatively simple.

As wind speeds at Cape Verde are relatively constant, the most significant source of variability in infrasonic noise levels is the diurnal effect (Figure 6; left panel) which is predominantly due to day-night variations in the speed of the trade winds. Infrasonic noise levels are highly correlated with this effect and thus at any time of day, noise levels are quite easily predicted. Significant wind speed and noise level variations are common in the Azores in the early winter. The experiment in November and December of 1999 occurred at a time of advancing inclement weather. Toward the end of the experiment wind speed on Sao Miguel could increase from 1 to 6 m/s in a few hours. Commensurate noise power increases of 40 to 50 dB occurred.

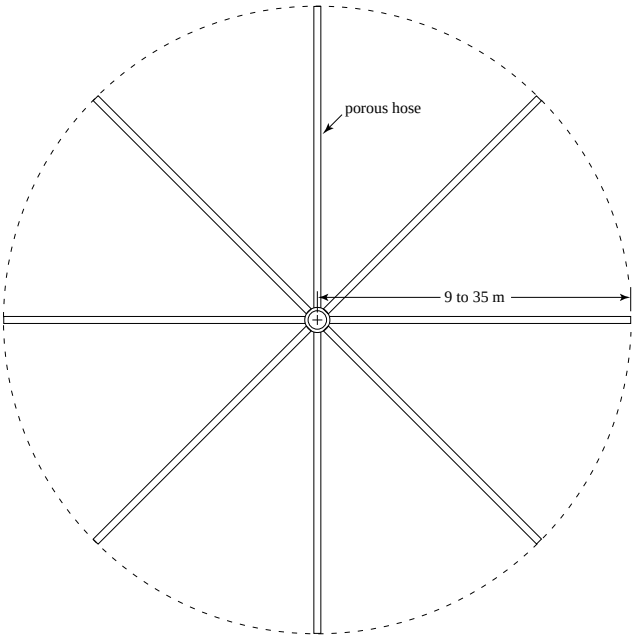

FIGURE 2. A "spider" Daniels filter. This filter is the simplest to construct and has a number of shortcomings. For example, the porosity is concentrated near the microbarometer at the center.

The Daniels Noise Space Filter

Daniels (1959) demonstrated that it is possible to increase the signal-to-noise ratio below 1 Hz by as much as 20 dB by averaging atmospheric pressure along a line. Daniels used a 1980 foot long tapered pipe along which pressure was sampled at 100 points. The success of this approach depends on the relatively small correlation lengths of infrasonic noise, which are due to local small-scale atmospheric turbulence, relative to the longer correlation lengths of infrasonic signals at the same frequencies. The linear porous pipe was useful for increasing signal to noise along a single azimuth perpendicular to the pipe.

Recent Approaches to Noise Reduction

The current monitoring situation is more complex than the one that existed in the 1950 s as we must now consider suspicious sources of any yield that occur at any location above or below ground. The global IMS network (Figure 1) will be used to detect weak signals detected with ever changing noise. The emphasis is on omnidirectional sensors and therefore the linear pipe arrangement is no longer adequate however the basic idea of sampling pressure over an area introduced by Daniels is still the basis of many modern noise reducing systems.

Various noise reducing devices have thus been recently proposed. A hexagonal arrangement of microporous pipes (Figure 7) was proposed in Paris at the 1998 infrasound workshop. Any system that employs micro-porous pipes averages pressure variations at a large number of points distributed along the pipes. The spatial extent of these systems is limited by the propagation of the signals from all ports to the summing manifold. These designs introduce phase delays and are limited to an aperture of ~ 1/4 of the wavelength (or ~75 m at 1 Hz). The hexagon design strives to overcome one limitation of the spider which concentrates most of the microporosity near the microphone. As illustrated in Figure 7, some hexagonal filters include several rings of porous pipe.

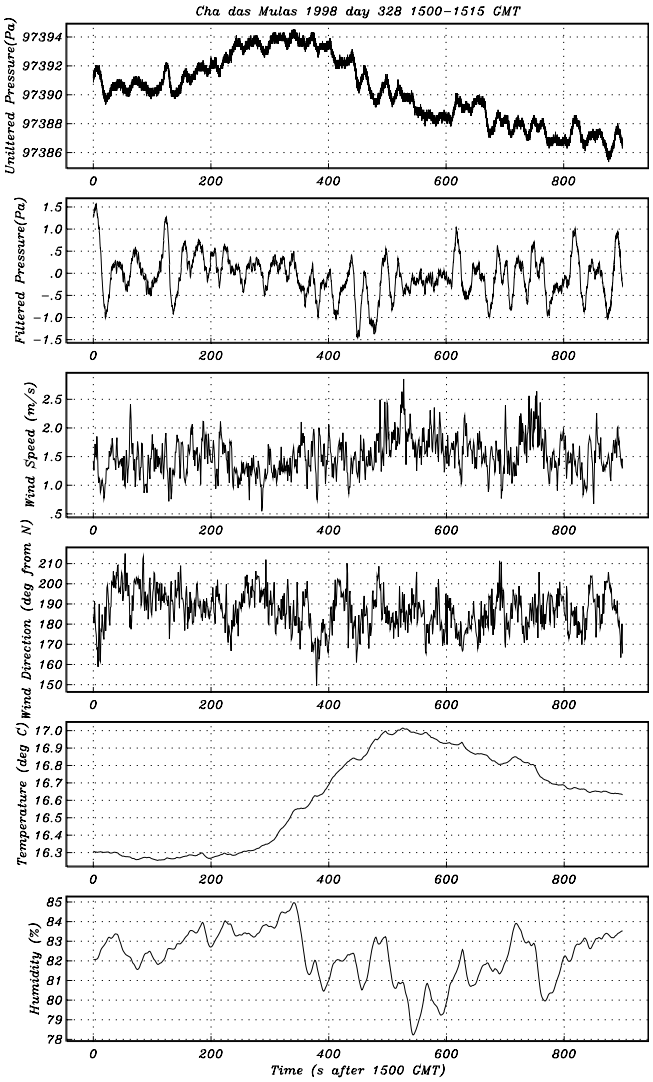

FIGURE 3. Atmospheric pressure and meteorological data from a 15 minute interval starting at 15:00 GMT at a site on Sao Miguel, Azores (Hedlin et al., 1999). Raw and filtered pressure data are shown in the upper two panels. Wind speed, direction, temperature and humidity are shown below. As shown in the next figure, this is a time of relatively low infrasonic noise.

A new design which involves discrete ports was conceived by Benoit Alcoverro at the Departement d'Analyse et de Surveillance de l'Environnement (DASE). This space filter distributes low-impedance ports spatially and signals are summed at a central manifold after propagation through impermeable pipes (Figures 8 and 9). The key features of this design is that the propagation distance, and thus the time delay, from each port to the summing manifold is equal and thus phase delays are eliminated. The impedances between the ports and the primary summing manifold are the same for all ports. Doug Christie (PTS, CTBTO) has proposed several innovative space filters based on this idea. The space filters range from 92 ports distributed over an area 18 m across (Figure 8) to 144 ports covering an area 70 m across (Figure 9). The narrower filter is considered to be effective at high frequencies. The 70 m aperture filter is considered appropriate for windy sites that require long-period noise suppression.

The Wind Shelter**.**

An example of a wind shelter is shown in Figure 10. These drawings are courtesy of Ludwik Liszka at the Swedish Institute of Space Physics. The wind shelter is akin to a forest as it reduces wind speeds inside the shelter and reduces the scale of the atmospheric turbulence so that much of the acoustic energy that results is displaced beyond the frequency band of interest. The design features of a filter (including the shelter height and porosity) are dependent on conditions at the site (Doug Revelle, personal communication). For example, the height of the shelter is dependent on the roughness of the surrounding topography and local mean wind speeds. We are currently building a wind fence that is 2 m tall.

An Optical Fiber Sensor.

Work on an entirely new kind of infrasound sensor - an Optical Fiber Infrasound Sensor (OFIS)- is now underway at IGPP funded under a separate program by DTRA. The aim of all mechanical filters is to sample the atmosphere at a series of points and add their pressure signals mechanically by joining

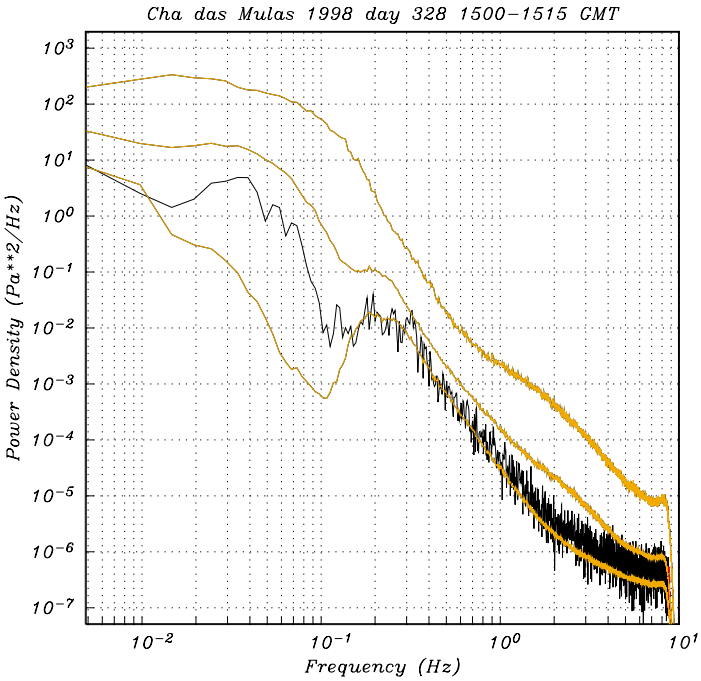

FIGURE 4. Noise power density at the Azores site. In black is shown a single power density estimate taken from the filtered pressure data displayed in the previous figure. The colored curves are the 10th, 50th and 90th percentile noise levels from the entire experiment. These curves are based on 454 noise level estimates taken at 1 hour intervals. Each estimate is taken from 15 minutes of data. The 5 second microbarom is not observed at times of high noise.

many tubes to a single microbarograph. Because of the finite sound velocity, there are phase delays along the lengths of the pipes, limiting the area that can be averaged over with mechanical filters. Further, because of the size of these spatial filters there is no practical way of measuring their response.

The Optical Fiber Infrasound Sensor (OFIS) consists of a long optical fiber whose optical path length is sensitive to the ambient atmospheric pressure. The OFIS integrates pressure variations that occur along the line in space defined by the optical fiber s path. The averaging characteristics are governed by the speed of light, so we can make the line over which pressure is averaged extremely long (many km). The distributed sensor approach has many advantages.

Figure 11 shows a schematic view of an OFIS. The optical path of a sensor fiber is interferometrically compared to that of a fiber shielded from the atmosphere. We have built two short test versions of the system. In one, we have added a mechanical element to the fiber which enhances its response to pressure changes.

In the context of the study proposed here, we have funding already to build an OFIS and deploy one version of it at Pinon Flat. The flexibility of an OFIS will allow us to readily rearrange it to sample over a configuration similar to one of the pipe arrays. Comparing records will allow us to assess the advantages of each and provide a method for determining the response of the acoustic filters.

OUTLINE OF OUR EXPERIMENT PLAN

The noise reduction systems we will investigate under our new DTRA contract are:

¥The porous hose spider (Figure 2).
¥The hexagonal porous pipe filter. (Figure 7)
¥An 18 m aperture multi-port filter. (Figure 8)
¥A 70 m aperture multi-port filter. (Figure 9)
¥A wind shelter. (Figure 10)
¥The Optical Fibre Infrasound Sensor (Figure 11)

All designs strive to provide omnidirectional noise reduction. The "Spider" design displayed in Figure 2 is commonly used in IMS infrasound surveys (e.g. those discussed in Hedlin et al., 2000). This is regarded as an inferior design. It is included to assess the performance of this simple filter relative to the more extensive, much costlier, filters. We are interested in constraining the performance jump the other (relatively expensive) systems will presumably provide over this simple filter and over a microbarometer that is not attached to any noise reduction device.

The hexagonal filter we will deploy at Pinon Flat will include ring at a radius of 9 m and two closely spaced rings at a radius of 35 m.

Theoretical work

The theory of sound propagation in pipes and networks of pipes is well developed through a combination of electrical analogs and the thermodynamics of air. The propagation properties of sound waves in enclosures such as pipes or volumes have a strong frequency dependence, due to the thermal and viscous boundary layers. This is in contrast to propagation properties in free air. The currently available accurate approximations of sound propagation in pipes and volumes span the entire frequency range of interest.

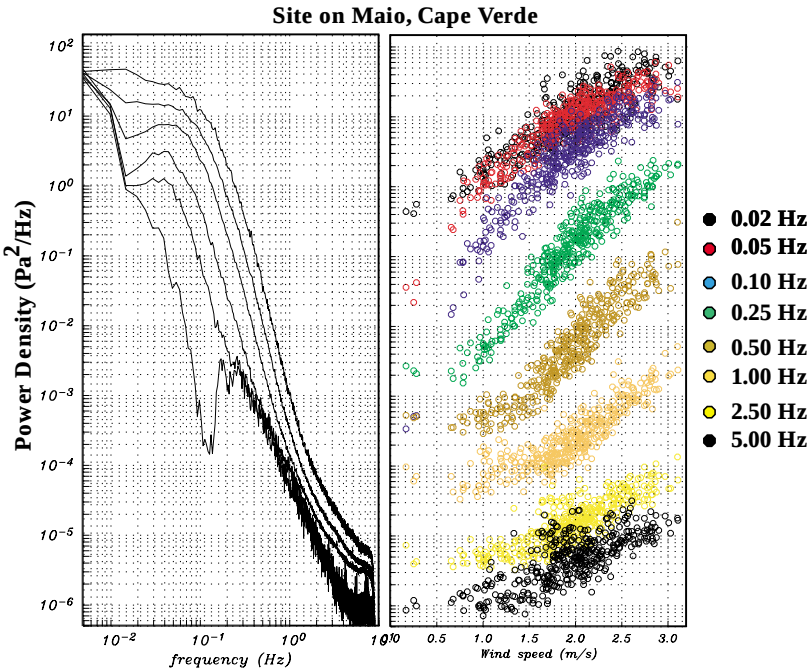

FIGURE 5. The panels to the left show the dependence of infrasonic noise power on frequency and wind speed at a site on Maio, Cape Verde. On the left we display average power spectral density as a function of wind speed. Infrasonic noise estimates were binned by wind speed into 0.5 m/s intervals starting at 0.0 m/s and then stacked. The curves on the left from lowest to highest are from the wind speed intervals from 0 to 0.5 m/s (lowest), 0.5 to 1.0 m/s (second lowest) up to 2.5 to 3.0 m/s (highest). On the right we display power spectral density from narrow frequency bands from the individual estimates. From top to bottom in each panel is noise power at 0.02 Hz (black); 0.05 Hz (red); 0.1 Hz (green); 0.25 Hz (dark blue); 0.5 Hz (light blue); 1.0 Hz (pink); 2.5 Hz (yellow); and 5.0 Hz (black).

In many of the earlier designs of noise-reducing structures at frequencies corresponding to the overall dimensions of the system, strong resonances occurred due to standing waves. Only through detailed impedance matching such resonances can be avoided. At higher frequencies the directional properties of most noise-reducers are increased, leading to an undesired departure from the omnidirectional angular response. In designing noise reducers one has to find a trade off between frequency response, angular response and the overall dimension of the system for the frequency band of interest (0.01 and 5 Hz).

Facilities.

The Pinon Flat Observatory is located about 100 miles from San Diego in the mountains that separate the coastal plain from the Imperial Valley (Figure 12). A section (1 square mile) is owned by the University of California as so provides plenty of space to deploy all of these systems simultaneously. It also provides basic infrastructure support such a lab space, accommodations, power, Internet connectivity, and security. An on-site caretaker is augmented by weekly visits by IGPP technicians.

As an environment for testing the efficacy of the various spatial filters, PFO offers a variety of wide wind conditions. As Figure 13 indicates we can expect a preponderance of wind speeds below 3 m/s however we can expect instantaneous wind speeds between 0 and 10+ m/s. Further there is a fairly uniform distribution of wind direction.

REFERENCES

Daniels, F.B. (1959), Noise-Reducing Line Microphone for Frequencies Below cps, J. Acoust. Soc. Am., **31**, 529.

Grover, F.H. (1971), Experimental Noise Reducers for an Active Microbarograph Array, Geophys. J.R. astr. Soc., **26**, 41.

Hedlin, M.A.H., Berger, J. and Vernon, F.L. (2000), Surveying Infrasonic Noise on Oceanic Islands, article in review with PAGEOPH.

Kaimal, J.C., and Finnigan, J.J. (1994), Atmospheric Boundary Layer Flows: Their Structure and Measurement, *Oxford University Press.*

McDonald, J.A., Douze, E.J., and Herrin, E. (1971), The structure of atmospheric turbulence and its application to the design of pipe arrays, *Geophys. J.R. astr. Soc.*, **26**, 99-109.

Panofsky, H.A., and Dutton, J.A. (1984) Atmospheric Turbulence: Models and Methods for Engineering Applications, *John Wiley and Sons Inc.*

Priestley, J.T. (1966), Correlation studies of pressure fluctuatinos on the ground beneath a turbulent boundary layer, Washington D.C., National Bureau of Standards Report No. 8942, U.S. Dept. of Commerce, National Bureau of Standard.

Wilson, D.K., Brasseur, J.G., and Gilbert, K.E. (1999), Acoustic scattering and the spectrum of atmospheric turbulence, *Journal of the Acoustical Society of America,* **105**, 30-34.

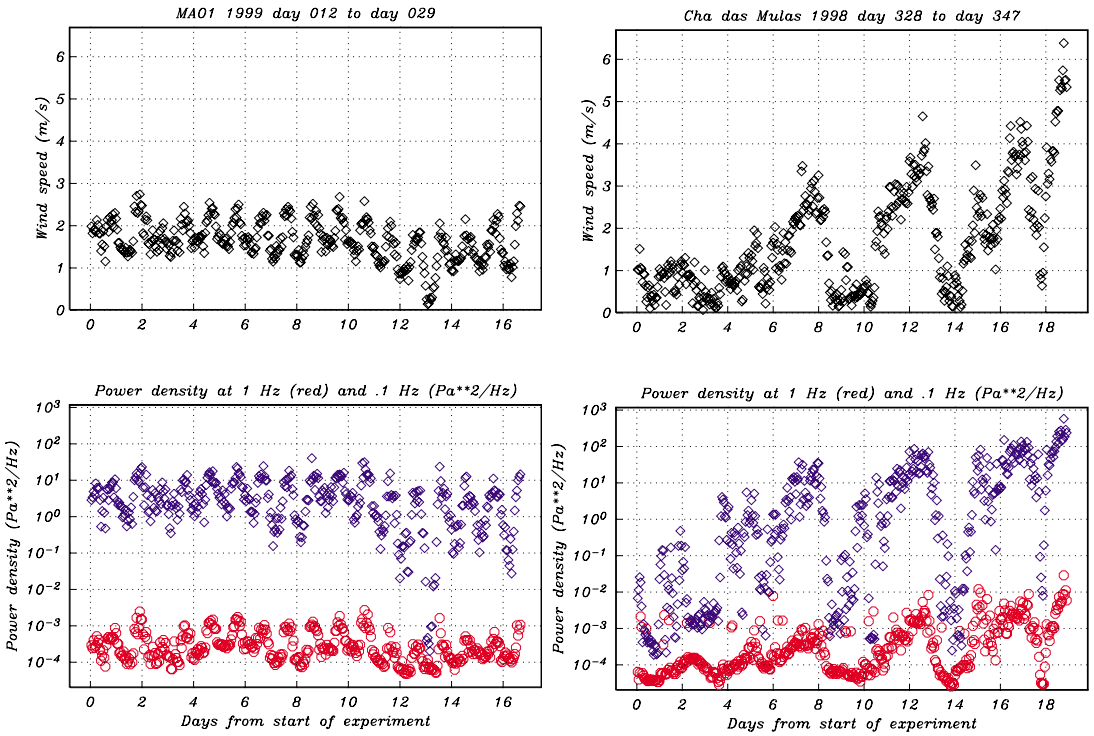

FIGURE 6. Noise power and wind speed as a function of time at one station in the Azores (left) and in Cape Verde. In the Azores, wind noise at 0.1 Hz (upper sequence of points in the lower panel) and at 1.0 Hz track closely the wind speed. Severe winds during a storm near the conclusion of the Azores experiment lead to wild swings in the noise level. At times, any infrasound station on the island will be deafened by the wind. In Cape Verde, diurnal variations are relatively slight.

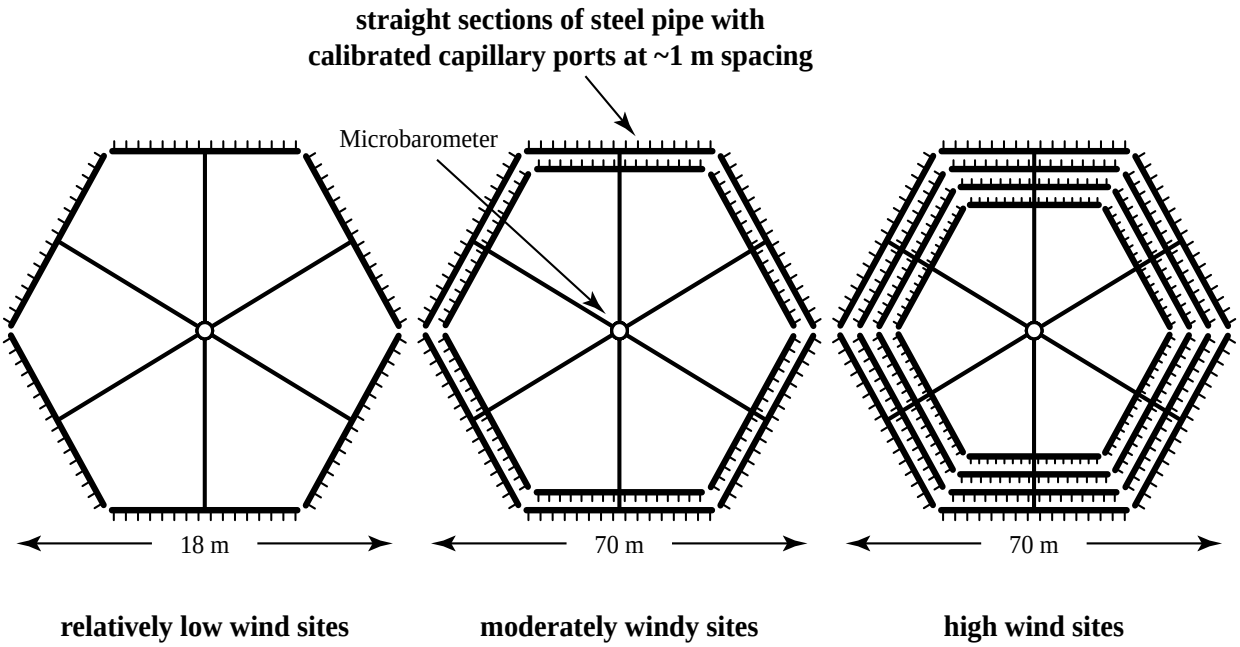

FIGURE 7. Three filters that use a hexagonal arrangement of porous pipes.

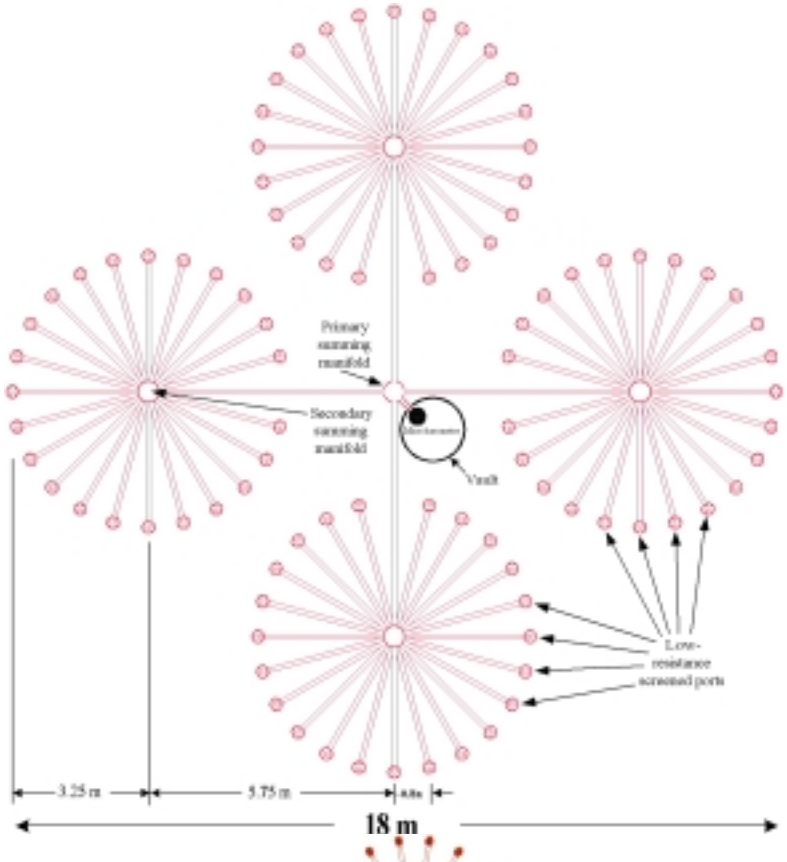

FIGURE 8. 92-port 18 m diameter wind-noise-reducing pipe array with high-frequency capability for use at short-period-optimized array elements at stations located in higher wind areas or at all array elements at stations located in low wind areas. This figure and caption are courtesy of Doug Christie.

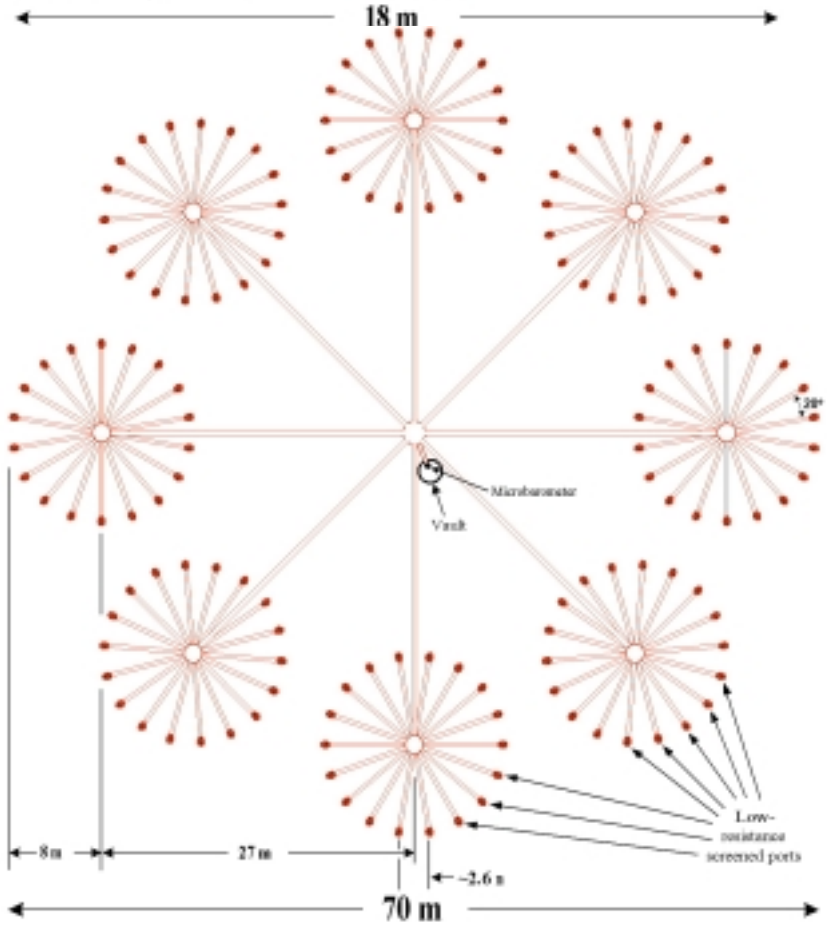

FIGURE 9. 144-port 70-m diameter wind-noise-reducing pipe array for use at long-period-optimized array elements at stations subject to high-wind conditions. Array and caption courtesy of Doug Christie.

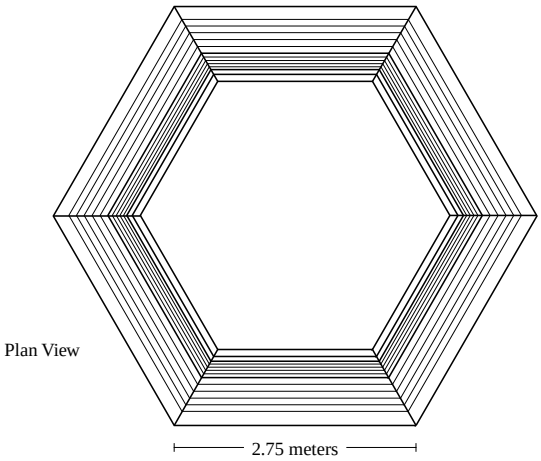

FIGURE 10. A wind shelter. This drawing was adapted from a sketch by Ludwik Liszka.

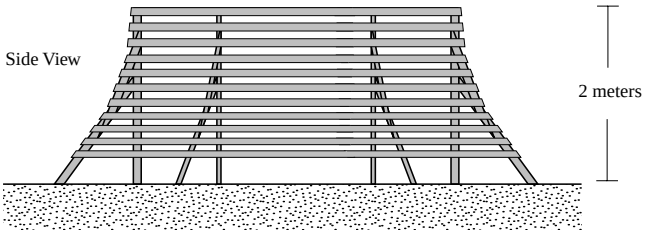

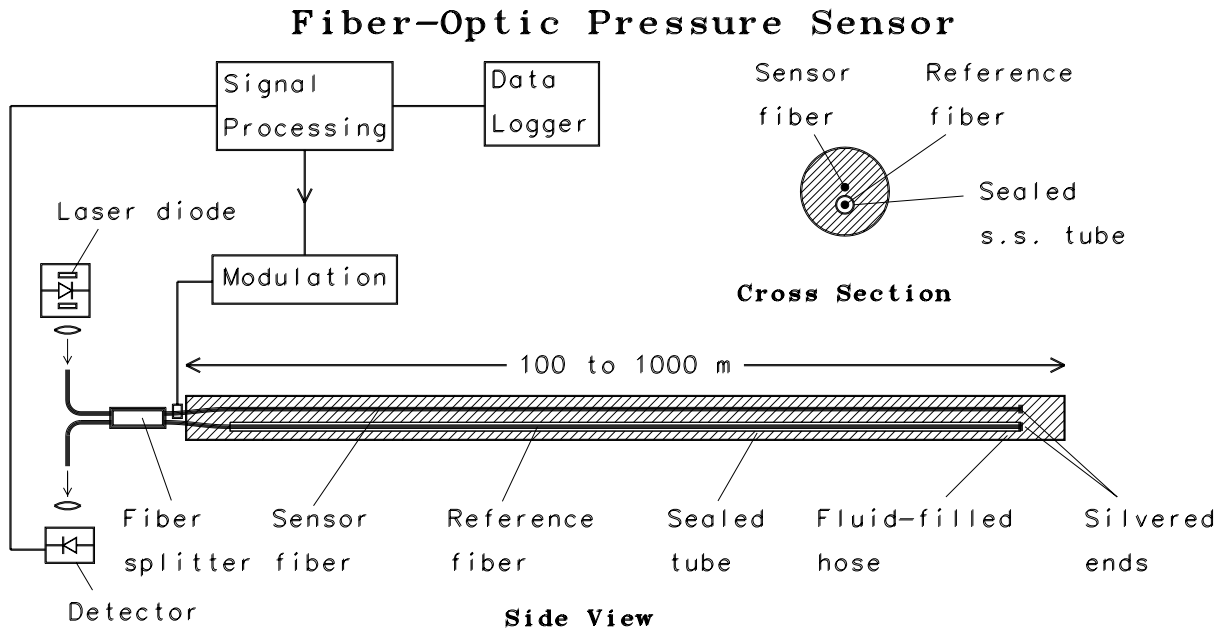

FIGURE 11. A schematic diagram of an Optical Fiber Infrasound Sensor (OFIS). Two optical fibers--one exposed to ambient pressure--form an interferometer. The integrated optical path length change caused by pressure variation along the sensor fiber is determined by the phase change of laser light traveling along the fiber. Temperature and laser wavelength fluctuations are common to both arms and largely cancel. Various schemes to increase the fiber's response to pressure changes and minimize response to strain and temperature are being investigated in our lab.

FIGURE 12. Pinon Flat Observatory . The photo, taken from the south shows a portion of one of the laser strainemeters

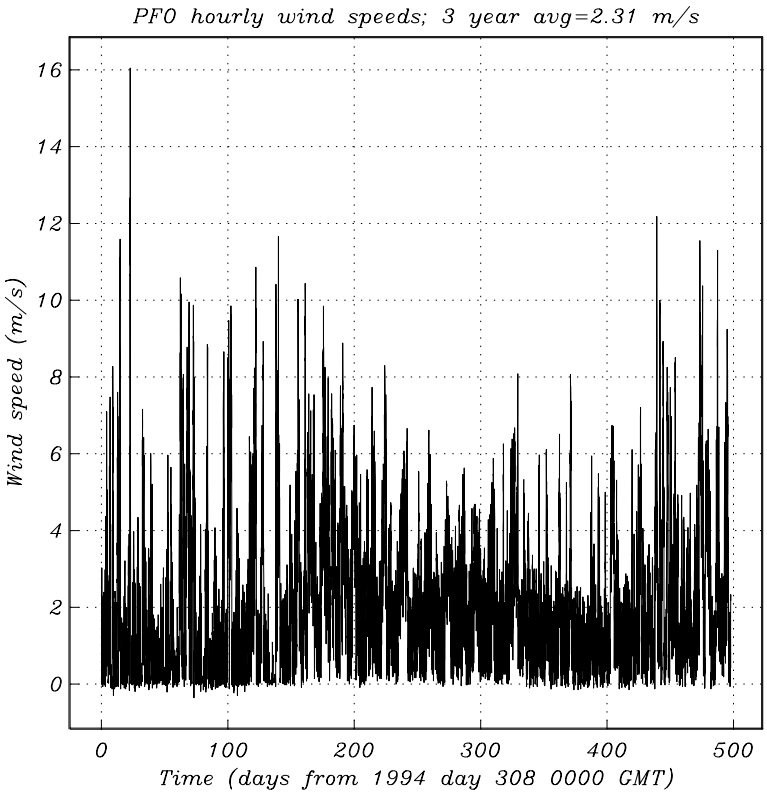

FIGURE 13. Instantaneous wind speed at an elevation of 2 m at the Pinon Flat Observatory for a 500 day time span starting on day 308 in 1994. These wind speed observations were taken once an hour.